MAPAN-JOURNAL ,
Publisher: METROLOGY SOC INDIA , NPL PREMISES,
Address: DR K S KRISHNAN MARG, NEW DELHI, INDIA,
ISSN / eISSN:0970-3950 / 0974-9853.
Volume 25-Issue 1-(2025)
https://doi-001.org/1025/17676264533007

OPEN ACCESS

Adaptive filter signal pressure detector in high density polyethylene water distribution networks to detect and locate leaks

Check for updates

Miloud Bentoumi [1], Ahmed Bentoumi [2]

[1] Laboratory of System Signal Analysis (LASS), Department of Electronics, Faculty of Technology, University of M'sila, University Pole, Road Bordj Bou Arreridj, M'sila 28000, Algeria, Email: miloud.bentoumi@univ-msila.dz

[2] University of M'sila University Pole, Road Bordj Bou Arreridj, M'sila 28000, Algeria, Email: ahmed_bentoumi@yahoo.fr

Received : 29/12/2025 ; Published: 05/01/2026

Abstract

The currently sold leak detectors worldwide are based on the analysis of acoustic emissions from pipeline leaks. Unfortunately, they not only detect pipeline leakage signals but also the noise from daily human activities and road traffic. These usually cause false alarms, resulting in damage to infrastructures when using these devices with inexperienced agents. In this study, the authors propose as a first contribution pressure transmitters, whose information is not influenced by environmental noise. In addition, for an arbitrarily chosen position of the pressure sensor, an analysis is carried out on the denoising quality as a function of the filter parameters for different denoising filters like EMD (empirical mode decomposition) and wavelet (WT). In our case, we opted for the adaptive filtering Kalman which presents a better metric signal-to-noise ratio of 46 dB like WT and EMD denoising. A novel detector based on adaptive filter signal pressure (AFSPD) is proposed to detect a leak. Many methods are utilized to know the leak's position, which generally depends on the proposed mathematical model. In our work two methods delay time and numerical cross-correlation are used to locate the leak relative to one of the transducers. In doing this, the validation of the detection and localization technique is confirmed by previously known positions, on the designed PEHD prototype pipe with a diameter of 40mm and a length of 100m. Furthermore, an acquisition system is based essentially on a DSpace professional research acquisition card and pressure transducers installed on the prototype pipeline.

KEYWORDS: WDNs, Pressure transducer, Kalman Filter, Leakage detection, Localization.

1. Introduction

Water distribution is an essential component of urban infrastructure, and is managed by government bodies or utilities responsible for ensuring that water is supplied regularly and safely to consumers [1]. This process generally involves the construction and maintenance of pipes, storage reservoirs pumping stations, and water quality control devices [2]. A certain amount of pressure is required to circulate water through the pipes [3]. If the latter decreases to a certain value (threshold), and with the existence of a leak, this can engender contamination of the public [4]. Water pressure in the distribution network can also cause damage to infrastructure, as well as significant water losses that are costly for the company. High water pressure can exert a force on pipe walls, causing them to crack or break. Leaks can also be caused by accidents such as construction work in the vicinity of the distribution network [5]. These problems can degrade the quality of the water and cause health problems for those who use it. In addition, leaks lead to waste of drinking water which has become so precious, which has economic and environmental implications [6]. Water leak detection is the process of confirming and identifying leaks in water distribution systems. This can be achieved by using specialized such as modern or conventional water leak detectors. These devices can detect several parameters, such as changes in water pressure, noise, temperature, or flow rate, which can help to indicate the presence and location of a leak [7]. In this work, we thought to solve the leakage problem by changing the acoustic sensors which have the disadvantage of capturing the surrounding noise in general. The latter is detected by the majority of current acoustic and vibration detectors and generally causes false alarms annoying the infrastructures by the use of pressure transmitters [8]. These have the advantage of being very precise, and their information is not influenced by environmental noise [9]. To this end, we designed a new prototype pipe 100 meters long and 40 mm in diameter, on which our transducers are installed, as well as an acquisition system based essentially on a DSpace MicroLabBox professional research acquisition card [10]. The information given by the transducers is established by an integrated 4-20mA current loop [11]. Furthermore, the information transmitted by devices is always immersed in noise, whatever their type (digital or analog) [12]. For this, filtering (denoising) is essential. Several filtering techniques are available. We studied for a single distance from the second pressure transducer the effect of filtering parameters on the denoising of our signal using the SNR metric. At first, in the case of denoising by the KALMAN filter, we studied the effect of the variation of statistical quantities such as covariance of the signal on the efficiency of the filtering by calculating the SNR metric parameter. We fixed the covariance of the process noise which describes the error in predicting the future state of the system and varied the covariance of the measurement noise which describes the error in actually measuring the state of the system and vice versa. We also investigated wavelet denoising by initially using a specific type of

Daubechies wavelet, adjusting the wavelet level, and then calculating the signal-to-noise ratio (SNR). Next, we maintained a constant level while varying the wavelet order from Db2 to Db14. Finally, we systematically altered the wavelet type and computed the SNR. Ultimately, we applied the EMD technique to denoise our signal, which involves breaking the signal down into intrinsic mode functions (IMFs) and a residue. We discarded the first IMFs that correspond to high-frequency signals while retaining the low-frequency signals. As a result, we achieved an SNR of approximately 46 dB at a distance of 76 meters. In our work, we opted for adaptive filtering (Kalman filter) which offers also a better signal-to-noise ratio like wavelet and EMD denoising [13]. A threshold of T=10% of the maximum value of the signal at the location of the transmitters is used to determine whether a leak is present. We used two methods to locate the leakage point of one of the transducers. Validation of the detection and localization technique is confirmed by previously known positions.

2. Background on denoising methods

We present in this section the filtering methods which are used in this paper.

2.1 Wavelet method

In signal processing and mathematics, a wavelet is a mathematical tool used for analyzing the frequency content of signals. In other words, Wavelet analysis allows the use of long time intervals where we want more precise low-frequency information, and shorter regions where we want high-frequency information [14]. One major advantage afforded by wavelets is the ability to perform local analysis. Wavelet analysis is capable of revealing aspects of data that other signal analysis techniques miss, aspects like trends, breakdown points, discontinuities in higher derivatives, and self-similarity. Wavelet analysis can often compress or de-noise a signal without appreciable degradation. A wavelet is a waveform of effectively limited duration that has an average value of zero. CWT is defined as the sum over all time of the signal multiplied by scaled, shifted versions of the wavelet function ψ.

$$C(scale, position) = \int_{-\infty}^{+\infty} f(t)\,.\,\psi(scale, position, t)dt \qquad (1)$$

The basic mathematical representation of a wavelet involves dilation and translation of a mother wavelet function. One commonly used wavelet function is the Morlet wavelet, often used in continuous wavelet transforms. The Morlet wavelet is defined as a complex exponential modulated by a Gaussian function.

The Morlet wavelet function can be expressed as follows:

$$\psi(t) = A.\exp(i.2\pi f_0 t)\,.\,exp - \frac{t^2}{2\sigma^2} \qquad (2)$$

Where: $\psi(t)$ is the wavelet function at time t. A is a normalization constant. i is the imaginary unit. f_0 is the nondimensional frequency parameter that controls the number of oscillations within the wavelet. σ is the standard deviation of the Gaussian window, controlling the width of the wavelet in the time domain.

The continuous wavelet transforms of a signal $x(t)$ using the Morlet wavelet is given by the convolution of $x(t)$ with the scaled and translated wavelet:

$$W_x(a,b) = \int_{-\infty}^{+\infty} x(t).\frac{1}{\sqrt{a}}.\ \psi^*\ \frac{t-b}{a}\ dt \qquad (3)$$

a: represents the dilation (scaling) parameter. b: represents the translation parameter. ψ∗ is the complex conjugate of the wavelet function

This integral is computed for various values of a and b to analyze the signal at different scales and positions in time.

In [1], we divided the vibratory time signal into small intervals or segments to consider the signal to be stationary over these intervals. We then applied the CWT wavelet transform to these segments. On the matrix of wavelet coefficients, he used the first thresholding to binarize the image obtained from the wavelet transform. We then added up the number of 1's after binarization. Finally, a second threshold is applied to confirm the presence or absence of the leak. Two performance criteria are used false alarm rate (FAR) and the success rate (SR) to detect leak.

2.2 Kalman filter

The Kalman filter is a signal processing and estimation algorithm widely used to estimate the state of a dynamic system from a series of noisy measurements [15]. It works optimally for linear models and Gaussian distributions. Furthermore, it operates iteratively and employs prediction and correction equations to estimate the system's state. These equations, although complex, fundamentally aim to find an optimal compromise between the prediction based on the dynamic model of the system and the actual measurements. This is achieved by using weighted averages that consider the uncertainty associated with each estimate. In other words, The Kalman filter tries to predict the state $x \in \mathbb{R}^n$ of the discrete-time process that is represented by the following linear stochastic difference equation:

$$x(k) = Ax(k-1) + W(k) \qquad (4)$$

Where $x(k)$ is the predicted state at time instant k, A is the state transition matrix that relays $x(k-1)$ to $x(k)$, and $W(k)$ is the process noise that is assumed to be Gaussian with zero mean and covariance Q. The state transition process model is paired with a measurement equation that enables to observe the state and can be described as follows:

$$y(k) = Hx(k) + V(k) \qquad (5)$$

Where $y(k) \in \mathbb{R}^m$ is the measurement vector at time k, H is the measurement matrix, and $V(k)$ is the measurement noise vector that is assumed to be Gaussian with zero mean and covariance R. The Kalman filter consists of two steps: the prediction and the update.

Prediction:

Predicted state estimate:

$$\hat{x}^-(k|k-1) = A\hat{x}^+(k-1|k-1) \qquad (6)$$

Predicted error covariance:

$$\hat{P}^{-}(k|k-1) = A\hat{P}^{+}(k-1|k-1)A^{T} + Q \qquad (7)$$

Update:

Kalman gain:

$$K_g(k) = P^{-}(k|k)H^{T}[P^{-}(k|k)H^{T} + R]^{-1} \qquad (8)$$

Updated state estimate:

$$\hat{x}^{+}(k|k) = \hat{x}^{-}(k|k-1) + K_g(Y(k) - H\hat{x}^{-}(k|k-1)) \qquad (9)$$

Updated error covariance:

$$P^{+}(k|k) = (1 - K_g H)P^{-}(k|k-1) \qquad (10)$$

In [15] the authors present a new approach for detecting sensor faults within WSNs for smart irrigation by combining an autoregressive model with a Kalman filter.

2.3 **EMD empirical mode decomposition method**

EMD [16] is a nonlinear and nonstationary time domain decomposition method. It is an adaptive, data-driven algorithm that decomposes a time series into multiple empirical modes, known as intrinsic mode functions (IMFs). Each IMF represents a narrow band frequency–amplitude modulation that is often related to a specific physical process.

2.3.1**The EMD algorithm**

The EMD decomposes a signal y_0(t) into a series of intrinsic mode functions (IMFs) which are extracted via an iterative sifting process. First, the local maxima and minima of the signal are connected, respectively, by cubic splines to form the upper/lower envelopes. The average of the two envelopes is then subtracted from the original signal. This sifting process is then repeated several times to obtain the first IMF that oscillates at relatively higher frequencies than does the residual signal that is obtained by subtracting the IMF from the original signal. Then, the residual is deemed as the input for a new round of iterations. In turn, subsequent IMFs with lower oscillation frequencies are derived using the same process and the newly obtained residue.

The result of the EMD is a decomposition of the signal into the sum of the IMFs and a residue r (t). That is,

$$y_0(t) = \sum_{m=1}^{n_m} c_m(t) + r(t)$$

where $n_m$is the number of IMFs.

3. Proposed AFSPD leak-detection

The proposed leak detector uses pressure transducers to capture the pressure signals. In doing this, the following sections start by describing the hydraulic plant prototype and then detail the proposed AFSPD leak-detection method.

3.1 Hydraulic plant prototype

The proposed detection system relies on the hydraulic plant given in **Fig. 1**. It consists of a water pipeline, a water pump, with (P=0.8Kw, flow =100l/min and RPM = 2850), a water tank, two pressure transducers, model 811FMA (pressure range 0-100 PSIG, accuracy $\pm 0.25\%\ FS$) and data acquisition hardware. We used a PEHD pipe manufactured in 2022 by PLAST TUBE in Setif, with a diameter of Ø=40 mm, pipe thickness =2.4mm, a length of 100 m, and a nominal pressure of PN 10. To ensure that the circuit is watertight, we will need to feed the circuit before starting the measurements, and make sure there are no leaks in our pipe. Technical specifications of a pipeline are given in **Tab.1.**

a

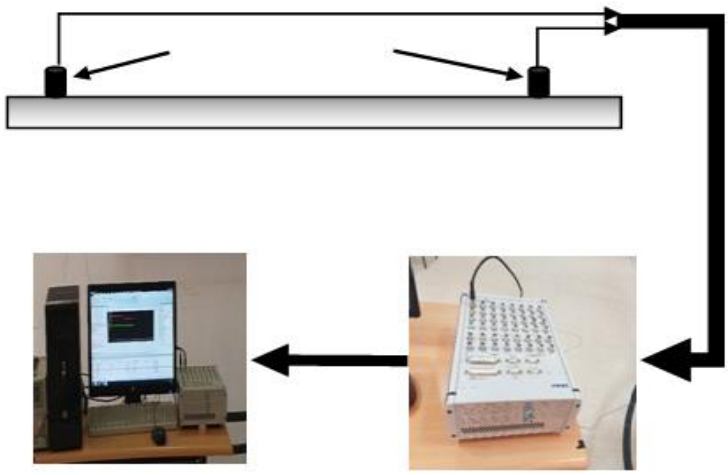

b

Fig.1 Hydraulic plant prototype for water leak detection with pressure transducers
(a) Image camera, (b) Corresponding block diagram.

Two pressure transducers spaced by a distance L are attached to the pipe. The position of the leak is initially taken at a distance of 15.5 m from the pump. The location of the transducers concerning the position of the leak is chosen in advance. We fixed one of the transducers at a position of 1.5m from the position of the leak. The other, we move it on the pipe, by distances of 1.5 m up to 78 m.

Measurements are taken as soon as a push-button is activated, simulating the leak. Recording times are set to a long duration of 20 seconds. Leakage is activated at approximately t =10s from the start of each recording. The leak is detected by a singularity in the acquired pressure signals. This singularity represents a depression in the pipe detected by the sensors. The pressure wave propagates on both sides of the leak and arrives at the transducers at different times.

Tab.1.Technical specifications of pipe

Characteristics and test methods	**PE 100**
Dimensional characteristics	**norm: NA 7700**
Fluidity index at 190°C-5Kg(g/10min)NA 357 /ISO 1113	**0,2 à 0,3 g/10 min**
Density NA 7603 /ISO 1183	**956Kg/m3**
Traction characteristics NA 7701 /ISO 6259	$\sigma_e \geq$ **19MPa ,** $\varepsilon_r \geq$ **400%**
Hot removal NA 7615 /ISO 2505	**≤ 3%**
Hydraulic pressure resistance NA 7517 / ISO 1167	**à 20°C** σ **= 12 MPa**
Oxidation stability à 210°C NA 7705 ISO 10837	**t ≥ 20 min**
Carbon black content NA 7665 /ISO 6964	**< 3%**
Roughness coefficient	**K=0.020mm**

To simulate a leak, we drilled a 12mm hole in the pipe. We did not leave the leak open to simulate the random nature of the event. In order to stimulate the latter, we used a solenoid valve controlled manually by a push button. The technical specifications of the solenoid valve are given by: power = 8 watts, Flow rate = 0.7 bar, Coil voltage =220 V. The overall electronic circuit is shown in **Fig.2**.

Fig.2 Electronic circuit.

Real-time control of the continuous system is via a PC connected with professional acquisition card **dSPACE DS1104.** The 4-20mA signals from pressure transmitters are small and are modeled by the equation [17].

I(mA) = 0.16 x **P(PSI) + 4mA** (11)

We need a conditioning stage to process them. By default, the Dspace acquisition card divides the input signals by 10. To recover the signal amplitude to its initial value a gain of 10 is necessary in the schematic Simulink of Matlab. To visualize the signals, we added another gain of 10. **Fig.3**. Furthermore, to process them we need to convert our signals using an analog-to-digital converter Which should be initially configured. We have chosen a sampling frequency of 1kHz. A build is required to obtain the executable file. The data files delivered by the acquisition device have a .csv and. mat extension and will be stored on the PC's hard disk.

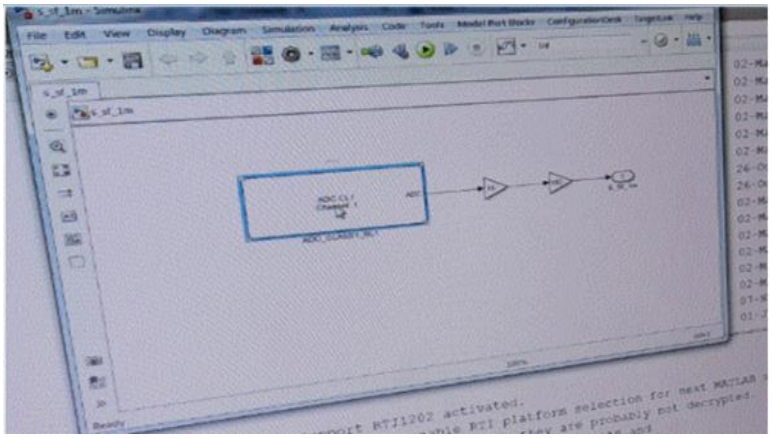

Fig.3 Simulink acquisition schematic.

3.2 Proposed detector AFSPD to detect leaks in WDNs

The two noisy signals $x_1(t) + n_1(t)$ and $x_2(t) + n_2(t)$ from the pressure sensors will be transformed into currents **Fig.4**.

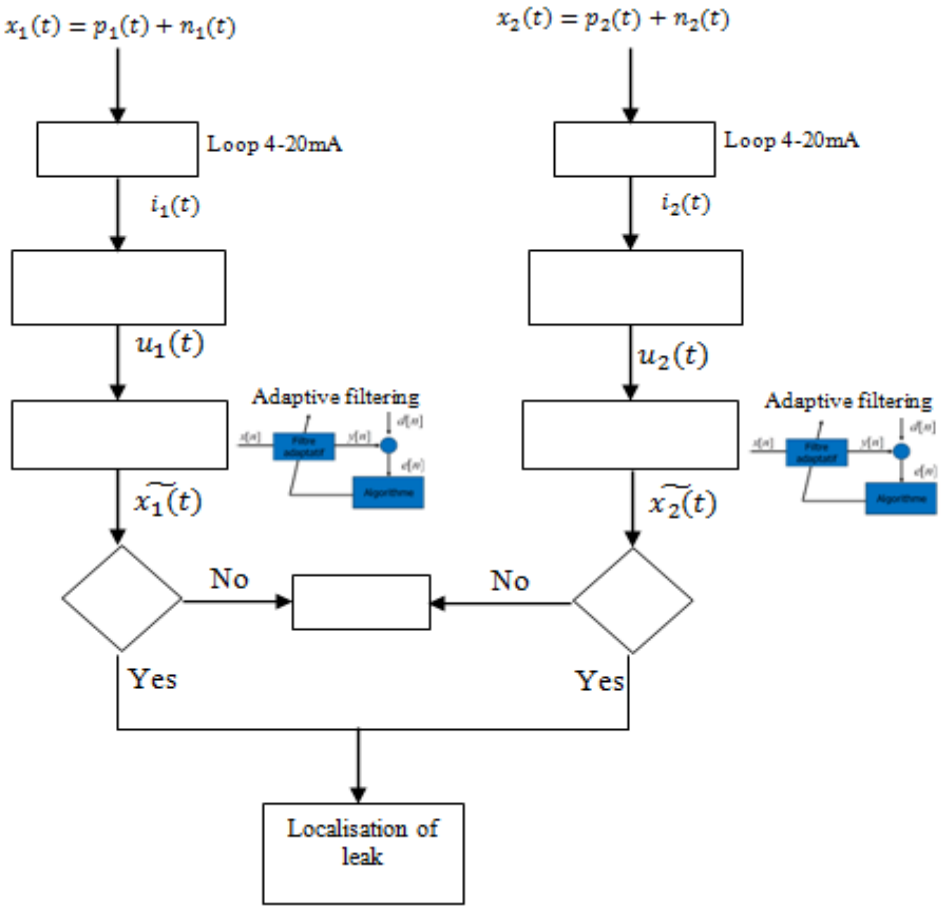

Fig.4 Proposed detector AFSPD .

$i_1(t)$ and $i_2(t)$ by a 4-20 mA loop because it is less susceptible to interference from electromagnetic fields and other sources of electrical noise and makes troubleshooting and maintenance more straightforward. A conditioning stage is needed to operate our signals. After this we obtained $u_1(t)$ et $u_2(t)$. An amplification of 100 is performed to upgrade our signals. To retain only relevant information, denoising is necessary. Several methods are available. We opted for adaptive filtering because of its performance. The estimated signals will be exploited to locate the position of the leak. The same threshold T=10% of pressure value from signals without a leak at the location where the transmitters are installed is applied on both estimate signals to confirm the presence of the leak and therefore the detection of the leak.

4 Experimental results and discussion

4.1 Signals without leak

Fig 5. Depicted the signals from the transducers in a randomly selected position when there is no leak. We notice that the pressures at the two transducer locations on the pipe, in relation to the pump, stay stable. The first pressure is approximately 167V, while the second is 147V. Additionally, we note that both signals are affected by noise.

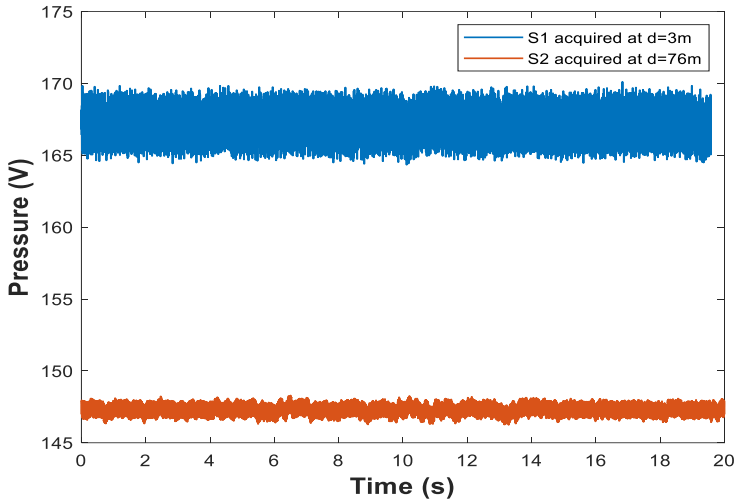

Fig 5. Pressure signals without leak.

4.2 Filtering study

Fig.6 shows the signals with and without leakage for a randomly chosen position. The position of the first transducer is 1.5m from the leak. Whereas the second transducer is taken at a position of 1m. The x-axis represents time in seconds and the y-axis represents pressure in volts.

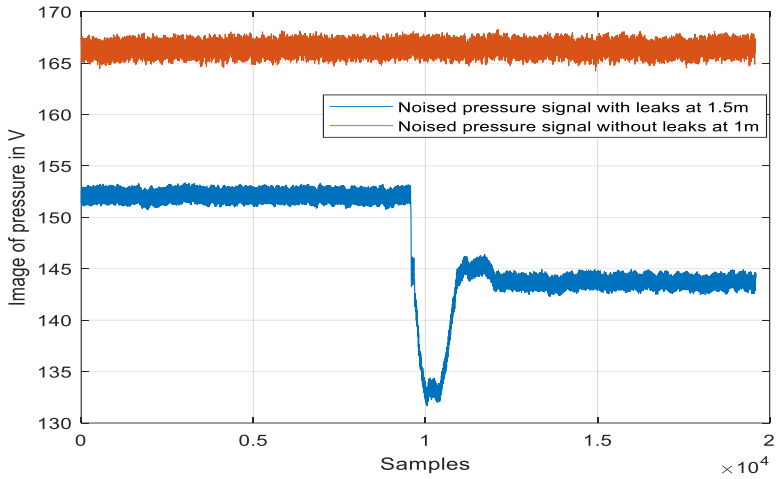

Fig.6 Noisy pressure signals with and without leak for Transducer1 =1m and Transducer2 =1 m.

The red signal represents the signal without a leak picked up by the transducer. The pressure image at this point in the pipe has an average value of 1.68V. We also note the random nature of the acquired signal, in other words, a superposition of pressure and noise. The constancy of the pressure value at this point is visible. On the other hand, the second signal in blue represents the signal with leakage. A singularity is noted. This occurred at t=9.8s. Note that our signal was stable at around 1.52V until the push-button was pressed at t =9.8s. Then a depression of up to 1.33V occurs. It gradually reaches an average value of 1.44V. Statistical parameters obtained from noise: a mean noise value of 0.3357 and a standard deviation of 0.5251.

Fig.7 displays the noisy pressure time signals from the two transducers in the scenario of a leaking pipe.

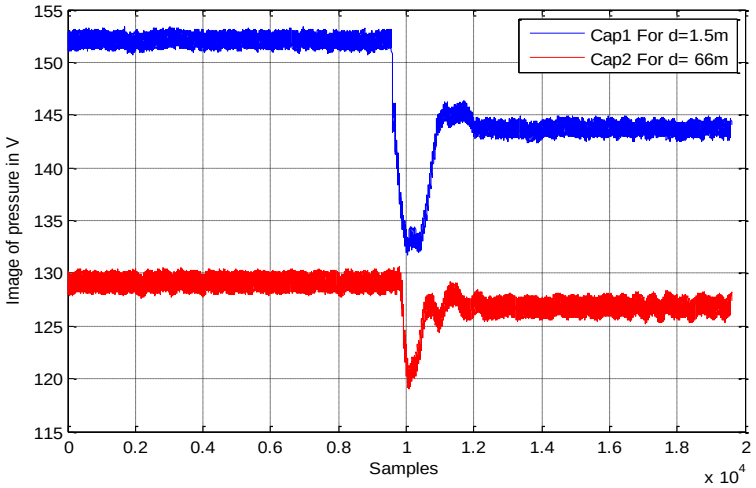

Fig.7 Time signals with leakage from the two pressure transducers.

Fig.7 illustrates two signals where leakage exists. The first transducer, which is nearer to the leak, recorded a significant drop of up to 1.33V. In contrast, the other transducer exhibited a less pronounced drop than the first, with a time shift of approximately $\Delta t = 0.2s$ relative to the first. We also note that both signals are affected by noise. For this, filtering is used.

a- Signal filtering using the Kalman filter.

To denoise the leakage signals from the transducers, a Kalman filter algorithm is applied to each signal. The results obtained for different values of Q (covariance of W(k)) and R (covariance of V(k)) are shown in **Fig.8**, **Fig.9, and Fig.10.**

1. Q=0.1 and R=2

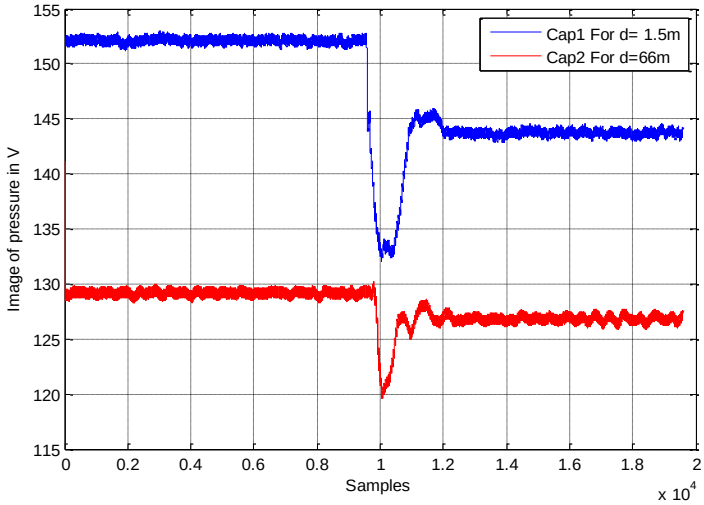

Fig.8 Denoising signals for Q =0.1 and R = 2.

By calculating the signal-to-noise ratio of the signals obtained after denoising and the noised signals, we found that SNR= 42.3638 dB.

At first, we chose values of Q=0.1 and R=2 we found our denoising was poor. We noticed a time lag between the transducer and the transducer signals representing that they arrive at the sensors at different times. At time t = 8,7 S, a depression is produced, signaling a leak detected by the sensor closest to the leak, and at time t = 9.9 S the depression phenomenon is detected by the second sensor.

2. Q=0.01 and R=4

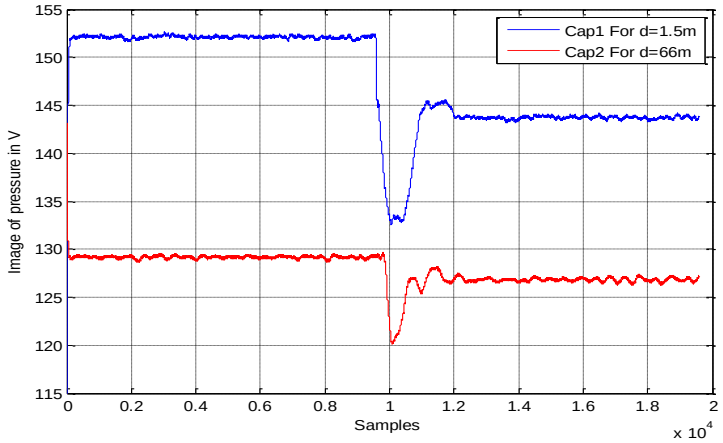

Fig.9. Denoising signals for Q =0.01 and R=4.

The SNR found for these Q and R values is SNR=37 .6829 dB. We can see that when we modified the Q and R parameters, we obtained relatively better denoising than the first, but not quite perfect, and the amplitude of the signal in the first transducer is greater than that of the second transducer as we found earlier. Note that as you move away from the pump, the pressure decreases.

3. **Q= 0.001 and R=6**

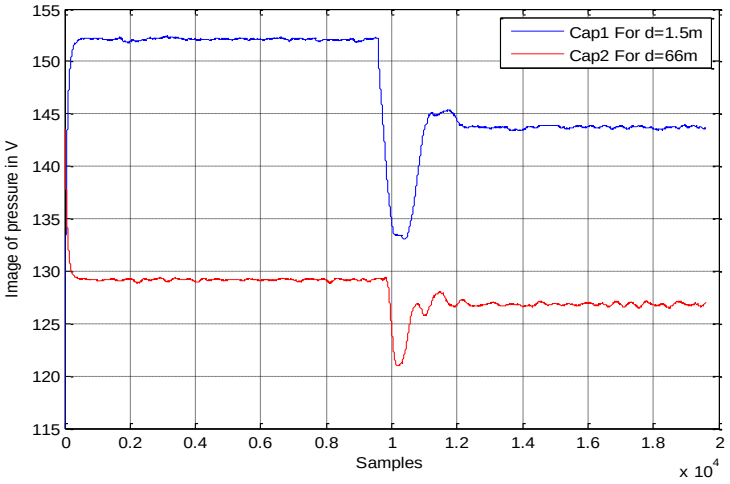

Fig.10 Denoising signals for Q =0.001 and R=6.

The SNR found for these Q and R values is SNR= 35.1442 dB.

In the latter case, when modifying the parameters Q and R by taking the values, Q =0.001 and R=6 we see better denoising, and from then on, we can say that the filtering of the two signals by the Kalman filter has been effective.

4.3 Calculation of Kalman filtering performance

To know the filtering performance of our signals, we used the SNR (Signal Noise Ratio) as a performance metric. To do this, we need to calculate the power of the signals, before and after filtering, and calculate their power ratios to determine their SNR and then in decibels (dB) over a given time window.

Signal power

$$P_S = \frac{1}{N}\sum x_i^2 \qquad (12)$$

Noise power: Noise power is obtained by subtracting the pre-filtering signal power from the post-filtering signal power. With the power of the signal after filtering.

$$P_B = \frac{1}{N}\sum x_i^2 - y_i^2 \qquad (13)$$

x_i et y_i are the noised and denoised signal samples respectively.

$$SNR_{dB} = 10.\log(\frac{P_S}{P_B}) \qquad (14)$$

The SNR we found for Q=0.001 and R=6 gave us better denoising.

a. Variation of SNR as a function of Q and R

The variation of SNR as a function of Q and R is shown in **Fig.11, and 12**.

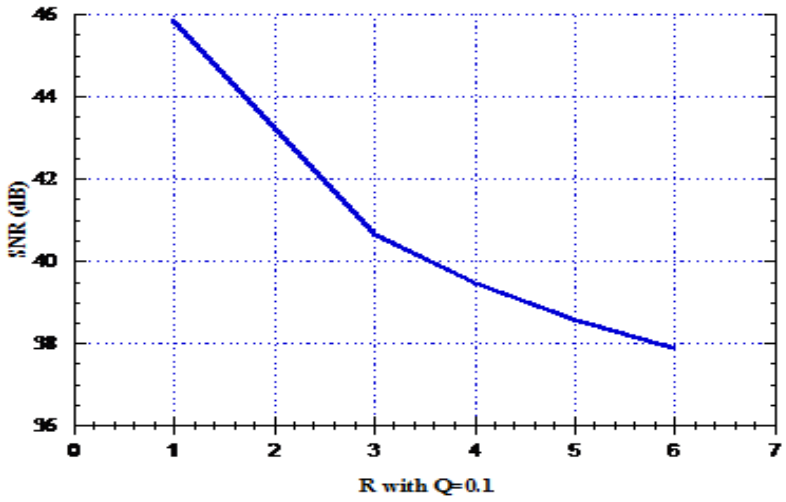

Fig.11 Variation of SNR as a function of R with constant Q.

In **Fig. 11**, we find that with a constant Q =0.1, the SNR gradually decreases with increasing R.

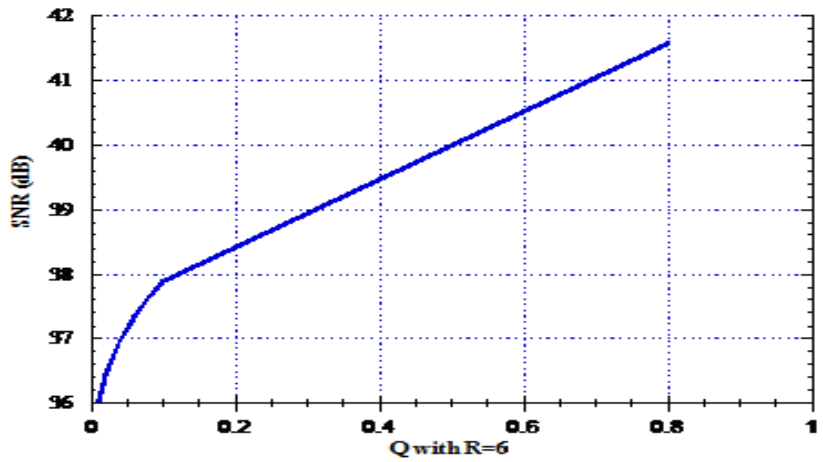

Fig.12 Variation of SNR as a function of Q with constant R.

4.4 Calculation of Wavelet Filtering Performance

When we use a wavelet, denoising performances are given below

In **Fig.13** we give the relation of SNR with levels for a Daubechies wavelet dB44.

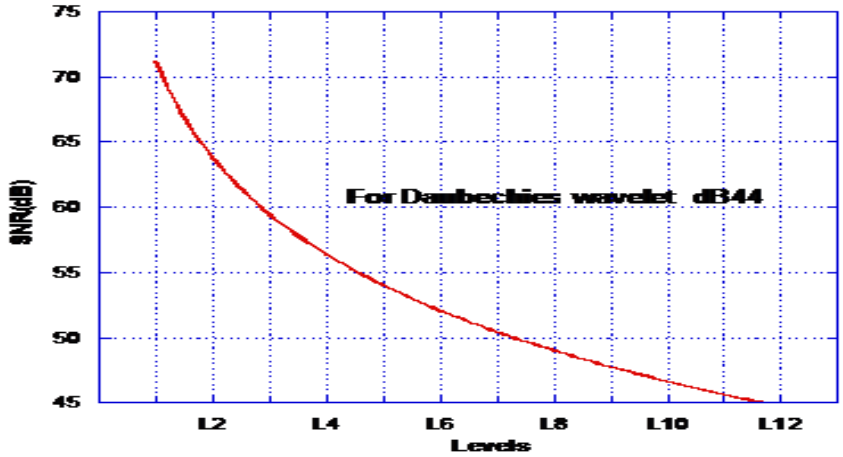

Fig .13SNR depending on levels **for wavelet dB44**

For a **Db44** wavelet type, the SNR decreases exponentially with wavelet level and can be modeled by the equation:

$$y = 71.153 - 24.472 \log x \qquad (15)$$

y represent the SNR in dB and x the level of this wavelet.

In **Fig.14** we give the relation of SNR with types of Daubechies wavelet for level 4.

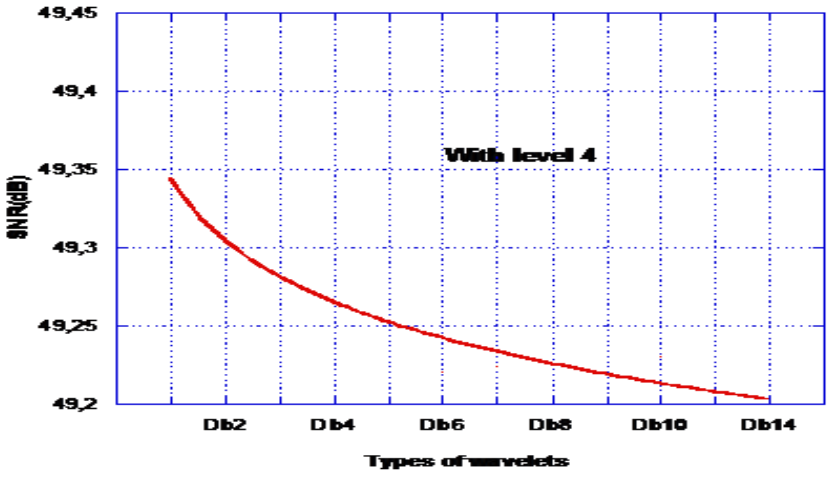

Fig.14 SNR with types of Daubechies wavelet for level 4.

For a 4-level wavelet Db type, the SNR decreases exponentially with wavelet type and can be modeled by:

$$y = 49.344 - 0.13092 \log x \qquad (16)$$

y represent the SNR in dB and x the Db type of wavelet.

Lastly, we gave a histogram of the SNR as a function of the wavelets. We found that the SNR is better when the FK4 wavelet is used **Fig.15**.

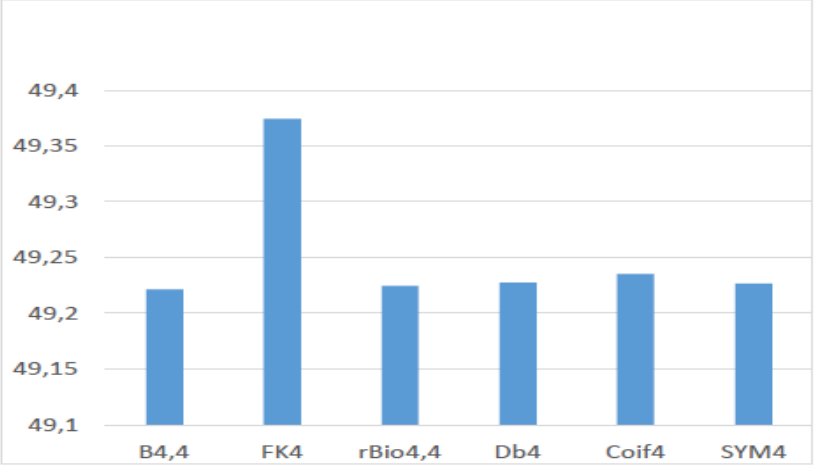

Fig.15. SNR as a function of the wavelets

4.5 Calculation of EMD Filtering Performance

Application of EMD to the noised pressure signal with leakage (NPSWL) at the distance of 76m **Fig.16**. gives IMFs. We have eliminated the high-frequency signals that represent noise (IMF1-IMF5) and the denoising pressure signal with a leak (DPSWL) is given in **Fig.17.**

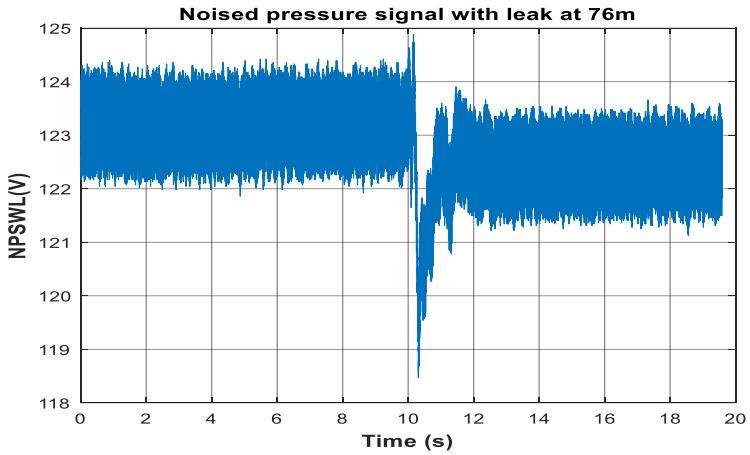

Fig.16 Signal with a leak at 76m

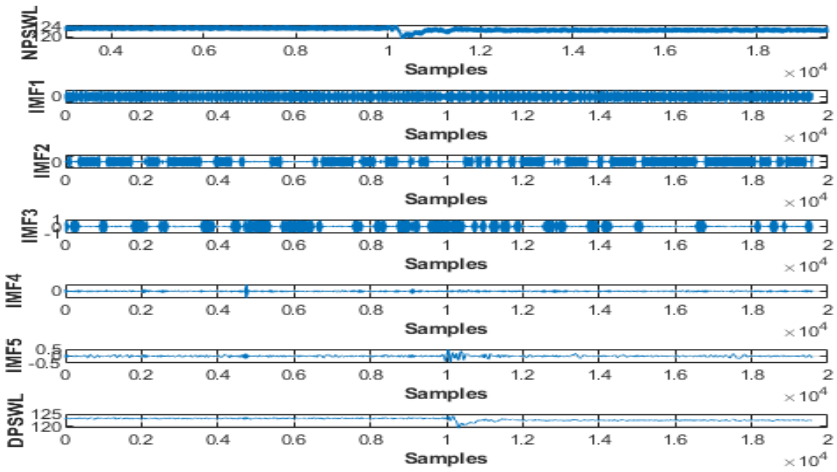

Fig.17 Noised(NPSWL) and denoised (DPSWL) pressure signal with leak and his IMFs .

We found the SNR=46.5144.

5 Localization of the leak position

Several methods are used to locate the leak to one of the transducers. These methods depend on the models proposed. In our case, two methods are used to determine the exact position of the leak to one of the transducers.

- By measuring experimentally, the lag time. Based on this, we can determine the position of one of the positions relative to one of the transducers.
- Using the inter-correlation function of the two filtered signals. The maximum of the inter-correlation function is used to determine the time lag which is used to calculate the exact position relative to one of the transducers.

5.1 Time lag calculated experimentally

This method involves determining the position of the leak to one of the transducers.

We have $X_1 = v.t_1$

And $X_2 = v.t_2$

Then $X_1 - X_2 = v.\Delta t$

And $X_1 - (L - X_1) = v.\Delta t$

So $2X_1 = L + v.\Delta t$

Finally

$$X_1 = \frac{L+v.\Delta t}{2} \quad (17)$$

The speed of propagation of the pressure wave in the last equation (18) can be obtained in two ways. It can be determined as the average of the speeds obtained from the measurements made, as well as from the equation given in the equation given in [18], where this pressure wave propagation velocity depends on pipe parameters such as pipe thickness and diameter.

$$v = \frac{1}{\sqrt{\rho(\frac{1}{K}+\frac{d}{eE})}} \quad (18)$$

v : Pressure wave propagation speed m/s

ρ : Liquid density= 998.2Kg/m^3

K: Modulus of elasticity of liquid=2.2*10^9 Pa

E: Young's modulus=9*10^{8}N/m^2

d: Internal pipe diameter =40 *10^{-3} m

e: Pipe thickness =2.4*10^{-3} m

Using the values characterizing the pipe, the calculated velocity value is**:** **v=229.785504m/s**

For predetermined distances, X_1 = 1.5m and X_2 =71.5m

Fig.18 the delay time (DT) found between them is 0.345s. This latter value is obtained by calculating the difference in the number of samples between the two signals and multiplying by the sampling time Δt =0.001s The average velocity found experimentally is v **= 202.8985507246 m/s**

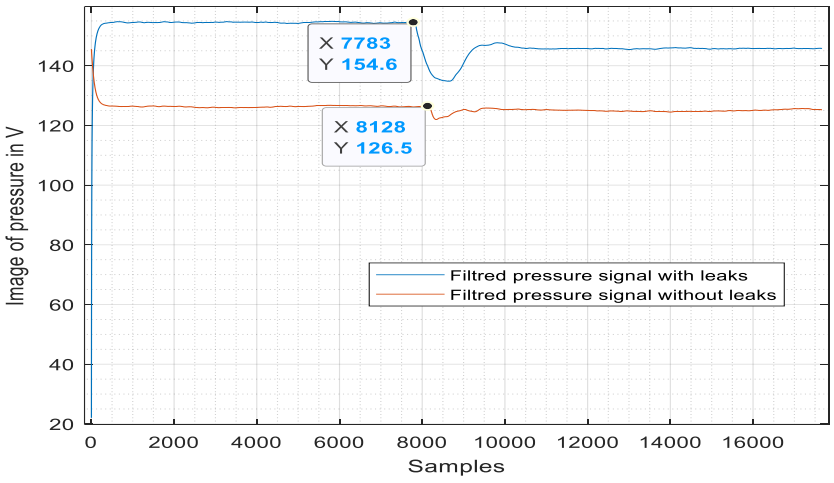

Fig. 18. Delay between the two signals for distances X_1 = 1.5m and X_2 = 71.5m.

For an arbitrary position, the acquired signals are depicted in **Fig.19**

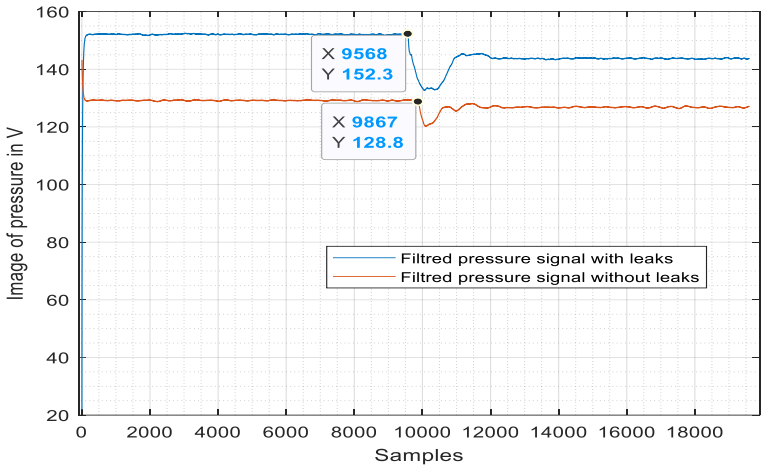

Fig.19. Delay between the two signals for X_1= 1.5m and X_2 =61m.

Knowing the speed, which is **v = 202.8985507246** m/s, and the DT found between the two signals is Δt = 0.299s. The distance found by calculation is X_1 = 60.666m, very near to the reel value of 61m.

5.2 Time lag calculated using numerical cross correlation

The DT can be obtained using another method, by calculating the numerical cross correlation (CN) of the two signals. The peak obtained is used to calculate Δt [19].

$$\Delta t = \frac{N-1-K_{pic}}{f_s} \qquad (19)$$

The K_{pic} is deduced from the curve in **Fig.20**.This makes it easier to determine the time lag and consequently the position relative to one of the transducers.

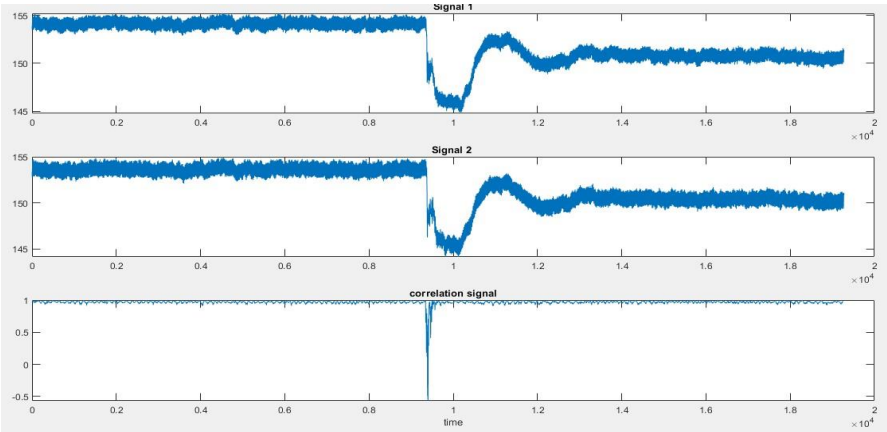

Fig. 20. Correlation result of the two signals.

Conclusion

In this work, we proposed an adaptive filter signal pressure detector (AFSPD) based on pressure transducers. Many filtering techniques are applied one is adaptive based on the Kalman filter and the other is based on wavelet transform and EMD. The quality of the filtering techniques adopted was studied based on signal-to-noise ratio (SNR). The results obtained are closer to the experimental values. They contain an error linked to the effective distance. The detector showed its effectiveness on a prototype pipeline.

References

[1]. Miloud Bentoumi, Djamel Chikouche, Amar Mezache, Haddi Bakhti 'Wavelet DT method for water leak-detection using a vibration sensor: an experimental analysis', IET Signal Processing, Volume 11, Issue 4, June 2017, pp: 349-493 DOI:10.1049/iet-spr.2016.0113

[2]. Bakhti, H., Bentoumi, M., Harrag, A., El-Hadi, K. (2019). Experimental validation of hybrid EMD-correlation acoustic digital leaks detector in water distribution network system. Instrumentation Mesure Métrologie,18(6): 535-545. https://doi.org/10.18280/i2m.180604

[3]. Miloud Bentoumi, Ahmed Bentoumi, Haddi Bakhti 'Welsh DSP Estimate and EMD Applied to Leak Detection in a Water Distribution Pipeline', Vol. 19, No. 1, February, 2020, pp. 35-41, DOI: 10.18280/i2m.190105

[4]. ChaimaCHABIRA , Haddi BAKHTI , Miloud BENTOUMI , Sabir MEFTAH , 'RNL used for the verification of the efficiency of a localization model in a real WDNs' The 2022 International Conference of Advanced Technology in Electronic and Electrical Engineering (ICATEEE) M'sila (Algeria) Year:2023 IEEE Xplore: 17 April 2023 DOI: 10.1109/ICATEEE57445.2022.10093092

[5]. Sabir Meftah;Miloud Bentoumi;Haddi Bakhti;Chaima Chabira 'Parameterization and Validation of the Physical Coefficients of a WDNs by BBO' The 2022 International Conference of Advanced Technology in Electronic and Electrical Engineering (ICATEEE) M'sila (Algeria) Year:2023 IEEE Xplore: 17 April 2023 DOI: 10.1109/ICATEEE57445.2022.10093730

[6]. Miloud Bentoumi;Haddi Bakhti;Chaima Chabira;Sabir Meftah 'S.G Filter And Speed of Pressure Wave Applied to locate leak in water pipe networks'The 2022 International Conference of Advanced Technology in Electronic and Electrical Engineering (ICATEEE) M'sila (Algeria) Year:2023 IEEE Xplore: 17 April 2023 DOI: 10.1109/ICATEEE57445.2022.10093689

[7]. Shuan Yan, Hongyong Yuan, Yan Gao, Boao Jin, Lizheng Deng, Kaiyuan Li, "Extracting acoustic leakage signals in buried pipes", Journal of Applied Geophysics, Vol 209,2023, https://doi.org/10.1016/j.jappgeo.2022.104918

[8]. Cuiwei Liu, Yuxing Li, Minghai Xu, "An integrated detection and location model for leakages in liquid pipelines", Journal of Petroleum Science and Engineering, Vol 2019, 2019; https://doi.org/10.1016/j.petrol.2018.12.078

[9]. Taghvaei, M., Beck, S.B.M., Staszewski, W.J. (2006). Leak detection in pipelines using cepstrum analysis. Journal of Measurement Science and Technology IOP Sciences, 17(2): 367-372, https://doi.org/10.1088/0957-0233/17/2/018

[10]. Lay-Ekuakille, A., Vendramin, G., Trotta, A. (2009). Robust spectral leak detection of complex pipelinesusing filter diagonalisation method. IEEE Sensors Journal, 9(11): 1605-1614. https://doi.org/10.1109/JSEN.2009.2027410

[11]. Martini, A., Troncossi, M., Rivola, A. (2015). Automatic leak detection in buried plastic pipes of water supply networks by means of vibration measurements. Shock and Vibration, 2015: 165304. https://doi.org/10.1155/2015/16530440

[12]. Gao, Y., Brennan, M.J., Joseph, P.F. (2006). A comparison of time delay estimators for the detection of

leak noise signals in plastic water distribution pipes. Journal of Sound and Vibration Elsevier, 292,pp: 552-570.
https://doi:10.1016/j.jsv.2005.08.014
[13]. Tang, X.H., Liu, Y.B., Zheng, L.J., Ma, C.B., Wang, H. (2009). Leak detection of water pipeline using wavelet transform method. International Conference on Environmental Science and Information ApplicationTechnology (IEEE), Wuhan, China. https://doi.org/10.1109/ESIAT.2009.57
[14]. Ahadi, M., Bakhtiar, M.S. (2010). Leak detection in water filled plastic pipes through the application of tuned wavelet transforms to acoustic emission signals. Applied acoustics journal Elsevier, 71(7): 634-639. https://doi.org/10.1016/j.apacoust.2010.02.006
[15]. Nassima Jihani, Mohammed Nabil Kabbaj, Mohammed Benbrahim, 'Kalman filter based sensor fault detection in wireless sensor network for smart irrigation', Results in Engineering journal, 7 September 2023 vol 20.
https://doi.org/10.1016/j.rineng.2023.101395
[16]. Yung-Hung Wang, Chien-Hung Yeh, Hsu-Wen Vincent Young, Kun Hu, Men-Tzung Lo, "On the computational complexity of the empirical mode decomposition algorithm", physica A journal, 400(2014), pp: 159-167,
http://dx.doi.org/10.1016/j.physa.2014.01.020
[16]. Zhang, L., Wu, Y.Z., Guo, L.X., Cai, P. (2013). Design implementation of leak acoustic signal correlator forwater pipelines. Information Technology Journal, 12(11): 2195-2200. https://doi.org /10.3923/itj.2013.2195.2200
[17]. OsTApkOwicz p. Leakage detection from liquid transmission pipelines using improved pressure wave technique. Eksploatacjai Niezawodnosc – Maintenance and Reliability 2014; 16 (1), pp: 9–16
[18]. Jian Li, Shili Chen, Yu Zhang, Shijiu Jin, Likun Wang 'Cross-correlation Method for Online Pipeline Leakage Monitoring System', IEEE conference 2009 2nd International Congress on Image and Signal Processing (CISP 2009), 17-19 October 2009, Tianjin, China, DOI: 10.1109/CISP.2009.5302839